Michael Hautmann

Effect of end-Triassic CO$_2$ maximum on carbonate sedimentation and marine mass extinction

Abstract Correlation of stratigraphic sections from different continents suggests a worldwide interruption of carbonate sedimentation at the Triassic–Jurassic boundary, which coincided with one of the most catastrophic mass extinctions in the Phanerozoic. Both events are linked by a vulcanogenic maximum of carbon dioxide, which led to a temporary undersaturation of sea water with respect to aragonite and calcite and a corresponding suppression of carbonate sedimentation including non-preservation of calcareous skeletons. Besides the frequently cited climatic effect of enhanced carbon dioxide, lowering the saturation state of sea water with respect to calcium carbonate was an additional driving force of the end-Triassic mass extinction, which chiefly affected organisms with thick aragonitic or high-magnesium calcitic skeletons. Replacement of aragonite by calcite, as found in the shells of epifaunal bivalves, was an evolutionary response to this condition.

Keywords Carbon dioxide · Calcium carbonate · Carbonate balance · Mass extinctions · Triassic · Jurassic

Introduction

Various extrinsic factors such as volcanism (Stothers 1993; Pálfy et al. 2002; Pálfy 2003), asteroid impact (Olsen et al. 1987; Ward et al. 2001) and sea level changes (Hallam and Wignall 1999) have been proposed as potential causes of the end-Triassic mass extinction, one of the five major extinction events in the Phanerozoic. However, sea-level changes fail to explain the terrestrial biotic crisis (Beerling 2002; Pálfy 2003), and potential impact craters and ejecta deposits predate the extinction

M. Hautmann (✉)
Institut für Paläontologie,
Universität Würzburg,
Pleicherwall 1, 97070 Würzburg, Germany
e-mail: hautmann@mail.uni-wuerzburg.de
Tel.: +49-0931-312511
Fax: +49-0931-312504

event by several million years (Walkden et al. 2002). By contrast, recent radiometric data corroborate that the eruptions in the Central Atlantic Magmatic Province (CAMP) were synchronous with the end-Triassic mass extinction (Pálfy 2003). The most frequently suggested link between CAMP-volcanism and mass extinction are rapid climate changes caused by volcanic outgassing of sulphur dioxide (SO$_2$) and carbon dioxide (CO$_2$; McHone 2003; Pálfy 2003). Total CO$_2$ emission by CAMP-volcanism has been estimated at 5.19×10^{12} metric tons (McHone 2003), i.e. about twice the total of Recent (pre-industrial) atmospheric CO$_2$. Additionally, a synchronous release of CO$_2$ from dissociated gas hydrates has been postulated to explain a carbon isotope excursion toward light values at the Triassic–Jurassic (T–J) boundary (Pálfy et al. 2001; Hesselbo et al. 2002). Evidence for enhanced atmospheric CO$_2$ has been found in reduced stomatal densities of land plants, which indicate that CO$_2$ increased from 600 ppm to 2100–2400 ppm across the T–J boundary (McElwain et al. 1999). Even higher CO$_2$ concentrations have been proposed on the basis of carbon isotope compositions of the Fe(CO$_3$)OH component in pedogenic oolithic goethites, which suggest a rise up to 18 times of the modern partial pressure of CO$_2$ (pCO$_2$), i.e. up to 5,990 ppmv (Yapp and Poths 1996). Calculation of the influence of high pCO$_2$ on the solubility of CaCO$_3$ in T–J sea water is complicated by uncertainties about palaeo-temperatures and ancient concentrations of the various dissolved ions (in particular Mg^{2+}/Ca^{2+} ratio). However, present-day sea water at a temperature of 25 °C would become undersaturated with respect to aragonite at pCO$_2$=10$^{-2.73}$ atm (1,860 ppmv) and with respect to calcite at pCO$_2$=10$^{-2.53}$ atm (2,950 ppmv; Stanley and Hardie 1998), thus within the same order of magnitude that has been suggested for CO$_2$ concentrations at the T–J boundary. Temporary suppression of marine carbonate production was therefore a potential consequence of the CAMP-volcanism.

Stratigraphy of the T–J boundary

Few continuous marine sections allow a more or less precise biostratigraphic determination of the T–J boundary. That of Queen Charlotte Islands (Canada) shows a shift from calcareous to siliciclastic sedimentation earlier than the T–J boundary defined by radiolarians, but the lithological change is accompanied by the disappearance of monotid bivalves and by a preservation change from body fossils to shell impressions (Ward et al. 2001). Similarly, there is a shift from carbonate to siliciclastic dominated sedimentation immediately above the highest occurrence of *Monotis* in northeastern British Columbia, starting with a hiatus at the upper surface of the top *Monotis*-bed (McRoberts et al. 2001; Orchard et al. 2001). In the section of St. Audrie's Bay, southwest England, the exact position of the T–J boundary is uncertain, but $\delta^{13}C$ excursions toward light values are invariably correlated with decreasing carbonate content (Hesselbo et al. 2002).

More precise biostratigraphic data are available in the classical sections of the Alps and in the candidate global stratotype sections of Nevada and Peru. In the Kendelbach Gorge (Austria) of the Alps (Fig. 1A), the base of the Jurassic is formed by an "unusual thick shale" overlying the calcareous beds of the Late Triassic Kössen Formation (Hallam 1981). This unit, also known as "Grenzmergel" (boundary marl), is actually free of carbonate (Hallam and Goodfellow 1990). It extends over more than 800 km from the western border of Austria, here known as the "boundary beds" (McRoberts et al. 1997), to the Tatra mountains (Carpathians) in Slovakia, where the non-calcareous "boundary clay" forms the base of the Jurassic (Soták 2003). The carbonates that underlay this widespread horizon locally show fissures and cavities that were originally interpreted as the effect of faulting and subsequent dissolution of aragonite under influence of freshwater (Furrer 1993), but submarine dissolution as a consequence of high $p\,CO_2$ may be an alternative interpretation. In the New York Canyon section (Fig. 1B), Nevada, USA, both biostratigraphy and geochemistry (negative $\delta^{13}C$ excursion) place the T–J boundary at the base of a siliciclastic intercalation between calcareous units (Guex et al. 2003), which probably is the equivalent of the clay horizon of the Alps and Carpathians. The Chambara Formation near Chilingote, Peru, is presently the only fully calcareous succession where ammonoid finds allow a relatively precise determination of the T–J boundary (Hillebrandt 1994). The first *Psiloceras* is found in a horizon originally interpreted as a tempestite (Hille-
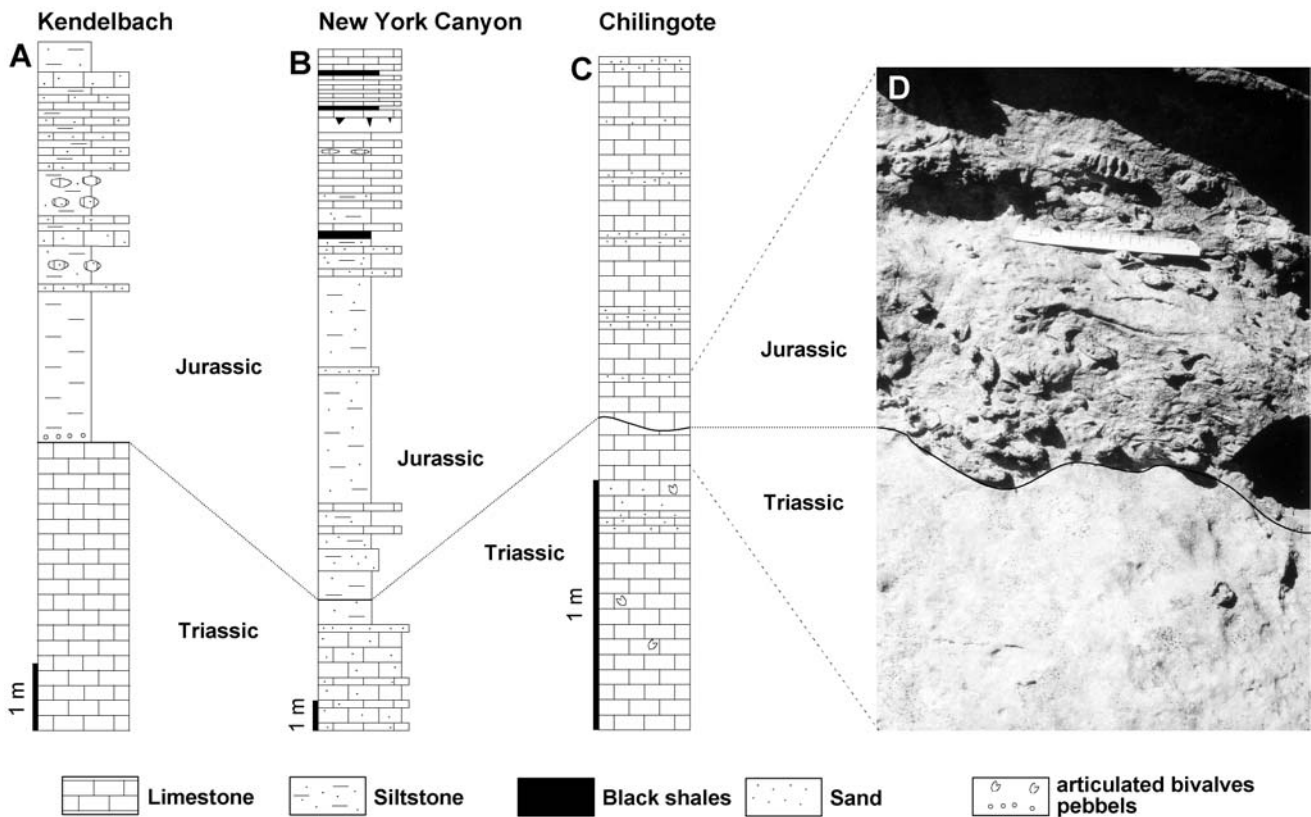
Fig. 1 T–J boundary sections from Europe, and North and South America. Position of T–J boundary taken from cited references. **A** Kendelbach Gorge, Osterhorn Mountains, Austria, exemplifying the abrupt change from carbonate to siliciclastic sedimentation in the Alps and Carpathians (Hallam and Goodfellow 1990). **B** New York Canyon, Nevada, USA, showing the same change in sedimentation in North America (Guex et al. 2003). **C** Chilingote, Peru, showing hiatus within the calcareous Chambara Formation (Hillebrandt 1994). **D** Detail of Chilingote section in field, photo by A. von Hillebrandt

brandt 1994), but a highly irregular base, a chaotic distribution of the fossils and the find of a reworked fragment of *Choristoceras* suggest that it is more likely a condensation horizon (Fig. 1C, D). The irregularity of the base resembles karstification but was obviously formed below sea level, because marine sedimentation continued in the siliciclastic Aramachay Formation, which is the landward equivalent of the Chambara Formation (Hillebrandt 1994). The discontinuity is therefore interpreted as a submarine dissolution surface that corresponds with the non-calcareous clay horizon that was simultaneously deposited in other regions.

In summary, the T–J transition is either found within a siliciclastic layer, which frequently marks an abrupt end of long-term carbonate sedimentation, or is represented by a hiatus in otherwise continuously calcareous sections. The concurrence of a worldwide interruption of carbonate deposition with a maximum in atmospheric CO_2 that was potentially high enough to dissolve calcium carbonate minerals is strong evidence for a causal linkage. Recent estimates of the duration of the T–J CO_2 maximum vary between >600,000 years (Hesselbo et al. 2002) and <100,000 years (Pálfy 2003). Taking standard sedimentation rates as starting point, a value near the lower extreme may be a good estimation of the time of duration, during which $p\,CO_2$ was high enough to suppress carbonate sedimentation. The inability to find a global stratotype section that provides a continuous record of calcareous fossils, in particular ammonoids, is probably an inevitable consequence of this non-actualistic condition.

## CaCO$_3$ undersaturation of sea water and marine mass extinction

The effect of increased $p\,CO_2$ on the carbonate saturation state of sea water and correlative consequences for carbonate secreting animals, in particular reef-forming corals, is of great interest for predictions of ecological and environmental changes associated with industrial CO_2 release. Smith and Buddemeier (1992) suggested that even in supersaturated conditions, lowering of the carbonate saturation state could cause a decrease in calcification, a shift towards calcite secretors, and/or a competitive advantage for non-calcifying reef organisms. Kleypas et al. (2001) calculated that doubling the pre-industrial CO_2 concentration in the atmosphere would decrease reef calcification by 14–30%, and they predicted that this drop would shift many reefs from net carbonate accumulation to net carbonate loss. Studies of extinction patterns of marine biocalcifiers during the time of the end-Triassic CO_2 maximum may provide clues to test such assumptions, which can not be verified by direct observations because they deal with non-actualistic conditions.

Assessing the relevance of CaCO$_3$ undersaturation of sea water for the T–J mass extinction requires a comparison between theoretically expected and actually observed effects. In sea water that is undersaturated with respect to calcium carbonate minerals, secretion of the least soluble polymorph would be a selective advantage because it requires the relatively lowest metabolic costs and provides the relatively highest resistance against dissolution. By contrast, organisms with aragonitic and high-magnesium calcitic skeletons are predicted to have suffered particularly high extinction rates, especially if their skeletons were thick. Replacement of aragonite by calcite is expected as an evolutionary response of animals that are pre-adapted to secrete both polymorphs, and size-reduction of the skeleton is a potential adaptation to the increased energetic costs for carbonate secretion.

Although it is not claimed that CaCO$_3$ undersaturation was the only mechanism that promoted the T–J marine mass extinction, extinction of aragonite- or high-magnesium calcite-secreting organisms clearly stands out from more random extinction of other groups. Most striking is the sudden disappearance of previously flourishing reef communities (Stanley 1988) that were nearly exclusively composed of organisms with thick aragonitic and high-magnesium calcitic skeletons. Accordingly, all major groups of reef organisms suffered high extinction rates, in particular aragonite-secreting spongiomorphs, inozoid and sphinctozoid sponges, tabulozoans, disjectoporids, scleractinian corals and involutinid foraminifers as well as high-magnesium calcite-secreting solenopores and *Tubiphytes* (Stanley 1988; Stanley and Hardie 1998). The severity of the end-Triassic extinction event for reef organisms is also expressed by an unusual long lag phase and a very slow recovery that did not start before the Pliensbachian (Stanley 1988).

Apart from reef organisms, extinction took the heaviest toll on aragonite-shelled mollusks. Most adversely affected were the ammonites, with no fewer than six superfamilies becoming extinct and possibly no more than one genus surviving the boundary (Hallam and Wignall 1997). The progressive decline through the Rhaetian that preceded the final extinction of many families (Hallam 2002) might have made them particularly vulnerable for an end-of-period *coup de grâce* caused by CaCO$_3$ undersaturation of sea water. The faunal turnover of gastropods is less well studied, but it has been proposed that it was even more pronounced than that at the end of the Permian (Batten 1973). Bivalves are worth a closer look because they are able to secrete both aragonite and low-magnesium calcite. Infaunal bivalves, which are invariably aragonite-shelled, were slightly more affected by the end-Triassic extinction event than epifaunal bivalves (McRoberts 2001), which frequently had partly calcitic shells. This pattern contrasts with higher extinction rates of epifaunal bivalves during the Triassic (McRoberts 2001), but any comparison between in- and epifauna might be inadequate because of the different chemical composition of pore and ocean water. However, epifaunal bivalve families that were particularly lightly affected by the end-Triassic extinction such as Ostreidae, Gryphaeidae, Plicatulidae, and Pectinidae, significantly enhanced the portion of calcite in their shell synchronous with the T–J CO_2 maximum (Fig. 2A). The Megalodontoidea,
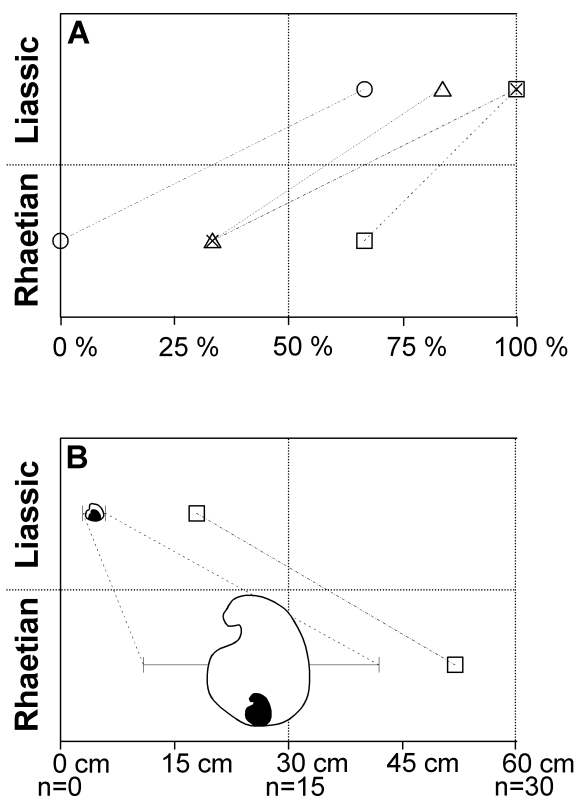
Fig. 2 Evolutionary responses of different clades of epifaunal bivalves to the end-Triassic CO_2 maximum. **A** Volumetric increase in shell calcite in the lineages *Indopecten - Pseudopecten* (Pectinidae; *circle*), *Eoplicatula - Harpax* (Plicatulidae; *triangle*), *Umbrostrea - Actinostreon* (Ostreidae; ×) and Triassic–Jurassic *Gryphaea* species (Gryphaeidae; *square*), based on data from Hautmann (2001a, 2001b), McRoberts and Carter (1994) and Carter (1990a, 1990b), assuming that outer, middle and inner shell layer take one third of the shell volume each. **B** Decrease in shell size in Megalodontoidea across the T–J boundary (minimum and maximum height of shell of adult individuals), shown numerically and by scaled outlines, and decrease in (sub)species diversity (*square*). Data taken from Végh-Neubrandt (1982) and own studies

which were the largest and most thick-shelled bivalves of the Late Triassic, retained their aragonitic shell but distinctly reduced their shell size (Fig. 2B). Yet, a strong decrease in their species diversity across the T–J boundary indicates that this strategy was less successful (Fig. 2B).

Replacement of shell aragonite by calcite at the T–J boundary was previously (Hautmann 2001a, 2001b) attributed to the shift from aragonite- to calcite-facilitating conditions in the oceans (Sandberg 1983). However, co-occurrence of calcitic and aragonitic ooides in the Rhaetian (Lakew 1990) and Liassic (Blomeier and Reijmer 1999) indicates that this transition was rather gradual, which is in contrast to the precise concurrence of shell mineralogical changes and the T–J boundary. Nonetheless, both phenomena may be linked: The end-Triassic CO_2 maximum obviously suppressed precipitation of both aragonite and calcite but exerted the strongest influence on organisms that built their skeletons by the more soluble polymorph. The apparently undirected pattern of

ooid mineralogy at the T–J boundary interval might have been caused similarly by pulses of lower CO_2 emissions that preceded and followed the boundary maximum and solely inhibited aragonite precipitation. By contrast, long-term oscillations between aragonite and calcite sea were probably triggered by gradual shifts in the Mg^{2+}/Ca^{2+} ratio, which led to the establishment of a stable "calcite sea" from the Middle Jurassic onwards (Stanley and Hardie 1998).

Conclusions

The lack of continuous fossiliferous sections across the T–J boundary has always been a major obstruction in analyses of the end-Triassic extinction event (e.g. Morante and Hallam 1996). Correlation of stratigraphic sections from Europe and North and South America demonstrates that this lack is attributed to a worldwide interruption of carbonate sedimentation at the T–J boundary, which includes the non-preservation of calcareous fossils. Its concurrence with the major volcanic activity of the Central Atlantic Magmatic Province and the corresponding atmospheric CO_2 peak suggests a causal linkage between volcanism, suppression of carbonate sedimentation and the end-Triassic mass extinction event. The mediating factor of enhanced atmospheric CO_2, which has repeatedly been suspected to have caused the end-Triassic mass extinction chiefly by extreme global warming (McElwain et al. 1999; Beerling 2002; Pálfy 2003), caused undersaturation of sea water with respect to aragonite and calcite and thereby suppressed carbonate deposition. Additionally, calcium carbonate undersaturation of sea water posed serious problems for marine carbonate secreting organisms that had to cope with raised energy expenditure for skeletal biomineralisation. This factor became critical for taxa with thick aragonitic and high-magnesium calcitic skeletons, which frequently failed to survive the T–J boundary. Size reduction and replacement of skeletal aragonite by calcite, as observed in several clades of epifaunal bivalves, were evolutionary responses to the non-actualistic chemical condition of sea water during the T–J transition.

References

Batten RL (1973) The vicissitudes of the gastropods during the interval of Guadalupian-Ladinian time. Canad Soc Petrol Geol Mem 2:596–607

Beerling D (2002) CO_2 and the end-Triassic mass extinction. Nature 415:386–387

Blomeier D, Reijmer JG (1999) Drowning of a Lower Jurassic carbonate platform: Jbel Bou Dahar, High Atlas, Morocco. Facies 41:81–110

Carter JG (1990a) Evolutionary significance of shell microstructure in the Palaeotaxodonta, Pteriomorphia and Isofilibranchia (Bivalvia: Mollusca). In: Carter JG (ed) Skeletal biomineralisation: patterns, processes and evolutionary trends, vol I. Reinhold, New York, pp 135–296

Carter JG (1990b) Shell microstructural data for the Bivalvia. In: Carter JG (ed) Skeletal biomineralisation: patterns, processes and evolutionary trends, vol I. Reinhold, New York, pp 297–411

Furrer H (1993) Stratigraphie und Facies der Trias/Jura-Grenzschichten in den oberostalpinen Decken Graubündens. Universität Zürich, Zurich, 99 pp

Guex J, Bartolini A, Atudorei V, Taylor D (2003) Two negative $\delta^{13}C_{org}$ excursions near the Triassic–Jurassic boundary in the New York Canyon area. Bull Géol Lausanne 360:1–4

Hallam A (1981) The end-Triassic bivalve mass extinction event. Palaeogeogr Palaeoclimatol Palaeoecol 35:1–44

Hallam A (2002) How catastrophic was the end-Triassic mass extinction? Lethaia 35:147–157

Hallam A, Goodfellow WD (1990) Facies and geochemical evidence bearing on the end-Triassic disappearance of the Alpine reef ecosystems. Histor Biol 4:131–138

Hallam A, Wignall PB (1997). Mass extinctions and their aftermath. Oxford Univ Press, Oxford, 320 pp

Hallam A, Wignall PB (1999) Mass extinctions and sea-level changes. Earth-Sci Rev 48:217–250

Hautmann M (2001a) Taxonomy and phylogeny of cementing Triassic Bivalves (Families Prospondylidae, Plicatulidae, Dimyidae and Ostreidae). Palaeontology 44:339–373

Hautmann M (2001b) Die Muschelfauna der Nayband-Formation (Obertrias, Nor-Rhät) des östlichen Zentraliran. Beringeria 29:1–181

Hesselbo SP, Robinson SA, Surlyk F, Piasecki S (2002) Terrestrial and marine extinction at the Triassic–Jurassic boundary synchronized with major carbon-cycle perturbation: A link to initiation of massive volcanism? Geology 30:251–254

Hillebrandt A von (1994) The Triassic/Jurassic boundary and Hettangian biostratigraphy in the area of the Utcubamba valley (northern Peru). Geobios 17:297–307

Kleypas JA, Buddemeier RW, Gattuso J-P (2001) The future of coral reefs in an age of global change. Int J Earth Sci 90:426–437

Lakew T (1990) Microfacies and cyclic sedimentation of the Upper Triassic (Rhaetian) Calcare di Zu (Southern Alps). Facies 22:187–232

McElwain JC, Beerling DJ, Woodward, FI (1999). Fossil plants and global warming at the Triassic–Jurassic Boundary. Science 285:1386–1390

McHone JG (2003). Volatile Emissions from Central Atlantic Magmatic Province basalts: mass assumptions and environmental consequences. In: Hames WE, McHone JG, Renne PR, Ruppel C (eds) The Central Atlantic Magmatic Province: insights from fragments of Pangea. Geophys Monogr Ser 136:241–254

McRoberts CA (2001) Triassic bivalves and the initial marine Mesozoic revolution: a role for predators? Geology 29:359–362

McRoberts CA, Carter JG (1994) Nacre in an early Gryphaeid bivalve (Mollusca). J Paleontol 68:1405–1408

McRoberts CA, Furrer H, Jones DS (1997) Palaeoenvironmental interpretation of a Triassic–Jurassic boundary section from western Austria based on palaeoecological and geochemical data. Palaeogeogr Palaeoclimatol Palaeoecol 136:79–95

McRoberts CA, Orchard ME, Hall R, Tozer ET, Zonneveld J-P (2001) Biochronology of the Triassic/Jurassic transition in northeast British Columbia, Canada. In: Hesselbo S (ed) IGCP 458 Triassic–Jurassic boundary events. SW England Field Workshop, Oxford, p 16

Morante R, Hallam A (1996) Organic carbon isotopic record across the Triassic–Jurassic boundary in Austria and its bearing on the cause of the mass extinction. Geology 24:391–394

Olsen PE, Shubin NH, Anders MH (1987) New early Jurassic tetrapod assemblages constrain Triassic–Jurassic tetrapod extinction event. Science 237:1025–1029

Orchard MJ, Zonneveld JP, Johns MJ, McRoberts CA, Sandy MR, Tozer ET, Carrelli GG (2001) Fossil succession and sequence stratigraphy of the Upper Triassic of Black Bear Ridge, northeast British Columbia: a GSSP prospect for the Carnian-Norian boundary. Albertiana 25:10–22

Pálfy J (2003) Volcanism of the Central Atlantic Magmatic Province as a potential driving force in the end-Triassic extinction. In: Hames WE, McHone JG, Renne PR, Ruppel C (eds) The Central Atlantic Magmatic Province: insights from fragments of Pangea. Geophys Monogr Ser 136:255–267

Pálfy J, Demény A, Haas J, Hetényi M, Orchard MJ, Vető I (2001) Carbon isotope anomaly and other geochemical changes at the Triassic–Jurassic boundary from a marine section in Hungary. Geology 29:1047–1050

Pálfy J, Smith PL, Mortensen JK (2002) Dating the end-Triassic and Early Jurassic mass extinctions, correlative large igneous provinces, and isotopic events. Geol Soc Amer, Littleton, Colorado, Special Paper no. 356, pp 523–532

Sandberg PA (1983) An oscillating trend in Phanerozoic non-skeletal carbonate mineralogy. Nature 305:19–22

Smith SV, Buddemeier RW (1992) Global change and coral reef ecosystems. Ann Rev Ecol Syst 23:89–118

Soták J (2003) High-nutrient conditions at the end of the Triassic period: the evidence of the last complex foraminifers and dasycladaceans from the Western Carpathians. In: Michalík J (ed) IGCP 458: Triassic–Jurassic boundary events. Third Field Workshop, Oxford, pp 33–34

Stanley GD (1988) The History of Early Mesozoic reef communities: a three-step process. Palaios 3:170–183

Stanley SM, Hardie LA (1998) Secular oscillations in the carbonate mineralogy of reef-building and sediment-producing organisms driven by tectonically forced shifts in seawater chemistry. Palaeogeogr Palaeoclimatol Palaeoecol 144:3–19

Stothers RB (1993) Flood basalts and extinction events. Geophys Res Lett 20:1399–1402

Végh-Neubrandt E (1982) Triassische Megalodontaceae. Entwicklung, Stratigraphie und Paläontologie. Akadémiai Kiadó, Budapest, 526 pp

Walkden G, Parker J, Kelley S (2002) A Late Triassic impact ejecta layer in southwestern Britain. Science 298:2185–2188

Ward PD, Haggart JW, Carter ES, Wilbur D, Tipper HW, Evans T (2001) Sudden productivity collapse associated with the Triassic–Jurassic boundary mass extinction. Science 292:1148–1151

Yapp CJ, Poth H (1996) Carbon isotopes in continental weathering environments and variations in ancient atmospheric CO_2 pressure. Earth Planet Sci Lett 137:71–82